



Surface functionalization induced enhanced surface properties and biocompatibility of polyaniline nanofibers

Journal:	<i>RSC Advances</i>
Manuscript ID:	RA-ART-01-2015-001809.R1
Article Type:	Paper
Date Submitted by the Author:	09-May-2015
Complete List of Authors:	Borah, Rajiv; Tezpur University, Physics Kumar, Ashok; Tezpur University, Physics Das, Monoj; Tezpur University, Molecular Biology and Biotechnology Ramteke, Anand; Tezpur University, Molecular Biology and Biotechnology

Surface functionalization induced enhancement in surface properties and biocompatibility of polyaniline nanofibers

Rajiv Borah¹, Ashok Kumar^{1,*}, Monoj Kumar Das², Anand Ramteke²

¹Materials Research Laboratory, Department of Physics, Tezpur University, Tezpur-784028, Assam, India

²Cancer Genetics and Chemoprevention Research Group, Department of Molecular Biology and Biotechnology, Tezpur University, Tezpur-784028, Assam, India

*Corresponding author's email: ask@tezu.ernet.in

Tel: +91-3712-275553

Abstract: In search of a novel bioactive platform for tissue engineering applications, nanofibers of Polyaniline (PAni) have been synthesized by dilute polymerization method and functionalized by 1% glutaraldehyde solution in phosphate buffer solution (PBS) solution ($P^H=7.4$) and in film form to introduce polar chemical group. TEM depicts size distribution of the nanofibers with an average diameter of 35.66 nm. FESEM images confirm nanofibrous structures with interconnected networks and highly entangled morphology of PAni powder and film, respectively. Thermogravimetric analysis indicates enhanced thermal stability of polyaniline nanofibers (PNFs) after functionalization. UV-visible absorption and photoluminescence studies depict that PNFs are in emeraldine base (EB) form before and after functionalization. FTIR and NMR spectroscopic studies reveal successful incorporation of polar hydroxyl (-OH) and aldehyde (-CHO) group functionality into PNFs. Contact angle measurements demonstrate an increase in wettability of PAni films after surface functionalization as contact angle decreases from 76.2° to 52.1° . Surface energy calculations along with its components using OWRK (Owens, Went, Rabel and Kaelble) and AB (Acid base) methods show increase in surface energy and surface polarity rendering surface biocompatibility to it. Membrane stability test reveals very less haemolysis activity of surface functionalized polyaniline nanofibers (SF-PNFs). MTT assay of human peripheral blood mononuclear cells (PBMC) shows significant increase in percentage of cell viability after surface functionalization of PNFs. Non-cytotoxic effect of SF-PNFs can make it a biocompatible scaffold for biomedical applications such as tissue engineering and drug delivery.

1. Introduction

Over the past few decades, one dimensional nanostructured materials in the fibrous form have been investigated with considerable interest due to their unique properties and high versatile applicability. Researchers across the world have been working in the field of tissue engineering to develop nanofibrous scaffolds for cell attachment and growth from biocompatible materials as nanofibrous materials are capable of providing 3D scaffolds for cellular activities, which are believed to behave like artificial extracellular matrix (ECM) [1]. Over the past two decades, electrically conducting polymers (CPs) have been investigated intensively as novel functional biomaterials due to their ability of highly specific physicochemical and biological functions of practical significance to improve current biomedical devices. These materials have attracted much interest because they display the physical and chemical properties of organic polymers and the electrical characteristics of metals [2] due to the formation of non linear defects such as solitons, polarons and bipolarons by the process of doping during polymerization. It has been reported that by using CPs, one can locally deliver electrical stimulus, provide a physical template for cell growth and tissue repair and allow precise external control over the level and duration of stimulation [3]. Past work has also demonstrated that electrical charges play an important role in stimulating either the cell proliferation or differentiation as it has been proved already that human body responds to electrical field and the key component of neural communication is the action potential generated at the synapse [3, 4]. Therefore, vast majority of recent research focuses on a wide range of biomedical applications of CPs including development of artificial muscles [5, 6, 7], controlled drug release [6], the stimulation of nerve regeneration [3, 6, 8, 9] and neural recording [3, 6].

Although the desired characteristics of a scaffold apart from electrical characteristics vary according to the native tissue, some general properties are inevitable. The foremost is the biocompatibility, meaning no immune response during integration with the host tissue [10]. The scaffold should also be porous to allow cell attachment and in growth as well as for exchange of nutrients during *in vivo* and *in vitro* culture. Also, as the scaffold is a temporary support, it should mimic native ECM both architecturally and functionally and in addition, it should be biodegradable.

In native tissues *in vivo*, normal cell behaviors attached on ECM are mediated by interaction between the ECM proteins like fibronectin, laminin, vitronectin, collagen etc. and the receptor proteins on the cell surface [11, 12]. The same principle is also applicable *in*

vitro in case of biomaterials, which act as mimic surface like ECM. It is believed that biomaterials interact with cells through adsorbed protein layers atop its surface [11]. The most important parameter of cell biomaterials interaction through adsorption of proteins is the surface hydrophilicity, which in fact allows covalent attachment of proteins atop materials' surface and presents normal bioactivity to the biomolecules. On the other hand, CPs are often considered as synthetic hydrophobic materials. Therefore, it is necessary to increase the hydrophilicity of the surface of CPs. It can be achieved through incorporation of polar groups like hydroxyl, carboxylic, aldehyde, amino and sulphate groups atop materials' surface. There are several methods available like plasma treatment by inert gas, irradiation by γ ray, electron beam, grafting copolymerization etc., which can enhance the hydrophilicity of biomaterials' surface [13].

Polyaniline (PAni) is one of the most mesmerizing CPs due to its diverse structural forms, ease of synthesis, high environmental stability and excellent charge transport property by doping/dedoping process. Availability of several such advantages has already placed it in many intriguing applications in wide range viz. electrochromic displays [14], rechargeable batteries [15], microelectronics [16], solar cells [17], sensors [18], actuators [18][19], electrorheological (ER) materials [20, 21] etc. It is also quite noticeable that the quest of area of applications of CPs including PAni has been directed recently towards diverse biomedical field. However, some serious issues like biocompatibility, biodegradability including unexpected side effects of bioactivity are of critical concern during biomedical application of these materials.

One of the major disadvantages of using PAni and its derivatives for biomedical applications arises from its apparently poor cell compatibility. However, Mattioli-Belmonte et al. were the first to demonstrate that this polymer is biocompatible *in vitro* and *in vivo* [9]. It has been reported PAni derivatives were found to be able to function as biocompatible substrates, upon which both H9c2 cardiac myoblasts and PC-12 pheochromocytoma cells can adhere, grow and differentiate well [4, 8]. Although biocompatibility of PAni has been reported earlier, we have reported here a simple method of functionalization of the surface of polyaniline nanofibers (PNFs) by using glutaraldehyde post to polymerization, as we reported in our earlier results [22]. This current research has been devoted to the incorporation of bioactivity to these synthetic materials' surface so that it can interact intentionally with the biological environment and influences the cell function. As discussed earlier, such kind of interactions can be often accomplished through surface modifications and incorporation of

polar groups, therefore, an attempt has been made to functionalize the surface of PNFs by introducing hydroxyl and aldehyde groups through glutaraldehyde. The detailed investigations after functionalization have been carried out by different characterization techniques such as TGA, FTIR, NMR, contact angle measurement, UV-visible and photoluminescence spectroscopy. The effect of surface functionalization on biocompatibility aspects has been investigated by membrane stability test and cell viability test of human peripheral blood mononuclear cells (PBMC) by MTT assay.

2. Surface energy calculations

Contact angle results have been analysed to determine surface energy and its various components by using Owens, Went, Rabel and Kaelble (OWRK) method [23] and Acid base (AB) method [24].

The OWRK method is used widely for calculation of total surface energy (γ) and its corresponding dispersive (γ^d) and polar (γ^p) components of polymeric materials taking two liquids of known γ^d and γ^p values. We have calculated total surface energy and its components taking water ($\gamma = 72.8 \text{ mNm}^{-1}$, $\gamma^d = 21.8 \text{ mNm}^{-1}$, $\gamma^p = 51.0 \text{ mNm}^{-1}$) and diiodomethane ($\gamma = 50.8 \text{ mNm}^{-1}$, $\gamma^d = 50.8 \text{ mNm}^{-1}$, $\gamma^p = 0$) using the following equations:

$$(\gamma_s^d \gamma_1^d)^{0.5} + (\gamma_s^p \gamma_1^p)^{0.5} = 0.5 \gamma_1 (1 + \cos \theta) \gamma_s^d \quad (1)$$

$$\gamma_s^d + \gamma_s^p = \gamma_s \quad (2)$$

Moreover, surface energy parameters including total surface energy of both the samples were calculated according to AB method of Van Oss–Chaudhury–Good theory [24, 25] as this method distinguishes the acid–base (AB) interactions as a component of the surface free energy as follows:

$$(\gamma_s^{LW} \gamma_1^{LW})^{0.5} + (\gamma_s^+ \gamma_1^-)^{0.5} + (\gamma_s^- \gamma_1^+)^{0.5} = 0.5 \gamma_1 (1 + \cos \theta) \quad (3)$$

$$\gamma_s^{LW} + \gamma_s^{AB} = \gamma_s \quad (4)$$

$$\gamma_s^{AB} = 2(\gamma_s^+ \gamma_s^-)^{0.5} \quad (5)$$

Where γ_s^{LW} and γ_l^{LW} = surface energy corresponding to Lifshitz–Van der Waals forces or dispersive components of solid and liquid respectively; γ_s^+ and γ_l^+ = Lewis acid components of solid and liquid respectively; γ_s^- and γ_l^- = Lewis base components of solid and liquid respectively; γ_s^{AB} = contribution of acid base interaction also refers to the polar component of solid surface.

It was performed by using contact angle data of three probe liquids: water ($\gamma^{LW} = 21.8 \text{ mNm}^{-1}$, $\gamma^+ = 25.5 \text{ mNm}^{-1}$, $\gamma^- = 25.5 \text{ mNm}^{-1}$) , ethylene glycol ($\gamma^{LW} = 29 \text{ mNm}^{-1}$, $\gamma^+ = 1.92 \text{ mNm}^{-1}$, $\gamma^- = 47.0 \text{ mNm}^{-1}$ and diiodomethane ($\gamma^{LW} = 50.8 \text{ mNm}^{-1}$, $\gamma^+ = 0.01 \text{ mNm}^{-1}$, $\gamma^- = 0$).

Percentage of polarity has been calculated using the following formulae:

$$\text{OWRK method: \% Polarity} = \frac{\gamma_s^p}{\gamma_s} \times 100$$

$$\text{AB method: \% Polarity} = \frac{\gamma_s^{LW}}{\gamma_s} \times 100$$

3. Results and discussion

3.1. Transmission Electron Microscopy

The average diameter of PNFs has been found to be 35.66 nm from transmission electron micrograph as shown in Figure 1. The SAED pattern depicts two little intensified diffused rings indicating semicrystalline/crystalline phase of PNFs, which is consistent with XRD results as shown in Figure S1 in ESI.

3.2: Scanning Electron Microscopy

Typical FESEM image of PNFs in powder form in Figure 2(a) demonstrates the nanofibrous structures of PANi with interconnected networks produced by dilute polymerization method. The fiber morphology of PNFs film prepared in NMP solution is shown in Figure 2(b). The morphology of the film suggests highly entangled aggregation among the nanofiber networks, which has been confirmed from its stability in solution more than one day and is in agreement with earlier reports [26, 27]. The thickness of the film is found to be approximately 30 μm .

3.3. Thermogravimetric Analysis

The thermal behaviour of PNFs and SF-PNFs has been investigated at a heating rate of 30⁰C/min under nitrogen atmosphere. The TGA thermograms and DTG plots of PNFs and SF-PNFs are shown in Figure 3(a) and (b). The weight loss below 100⁰C in both PNFs and SF-PNFs is attributed to the elimination of small amount of moisture [28]. Approximately, 5% weight loss occurs at 72⁰C for SF-PNFs and at 92⁰C for PNFs. The reason of higher weight loss at lower temperature in SF-PNFs than PNFs can be attributed to the presence of free glutaraldehyde molecules in addition of moisture on the surface of PNFs after functionalization. On the otherhand, the weight loss observed around 250⁰C is attributed to the evaporation of NMP solvent [29]. The thermogram of SF-PNFs shows a weight loss in the range of 335-355⁰C, which cannot be detected in PNFs. This may be due to the covalently bonded glutaraldehyde molecules in PANi chain. Before functionalization, PANi film shows a weight loss 23-25% and after surface functionalization with glutaraldehyde, it shows a weight loss of about 24-26% in the range of 335-355⁰C. Thereby, the estimated amount of actual glutaraldehyde incorporated onto the surface of PANi through covalent bonding is to be of about 1%. The major degradation temperature for the polymer backbone has been observed to be shifted from 519⁰C to 538⁰C after surface functionalization. This may be due to the different chemical structure of benzenoid and quinoid units in PANi chains after functionalization [29]. It is further clear from Figure 3(a) that PNFs lose 36% of their weight at 519⁰C, while SF-PNFs lose 37% of their weight at 538⁰C. It reveals that the weight loss corresponding to the PANi chains in SF-PNFs is slightly slower than that of PNFs, which leads to the improved thermal stability of the PANi after surface functionalization.

3.4. Spectroscopic Analysis

The features of electronic structures and relative conformational changes of PNFs before and after surface functionalization are probed by electronic absorptions in the UV-Vis region as shown in Figure 4. Two broad absorption bands in the region 300 nm and 600 nm appear in the absorption spectra of pristine and functionalized samples. The peak around 300 nm of PNFs is assigned to the $\pi-\pi^*$ band transitions, i.e., electronic transitions from the HOMO to LUMO and gives an idea of the band gap of the polymer [30]. This band transition peak is found to be blue shifted as compared to band transition peak at 330 nm for bulk PANi, confirming reduction in particle size. It is also attributed to the excitation of the benzenoid units in the polymer chain [30, 31]. In case of SF-PNFs, this peak appears with relatively

higher intensity. The other peak around 600 nm for the pristine and SF-PNFs, which is generally observed in the insulating EB form of the polymer ascribed to a local charge transfer between a quinoid ring and the adjacent imine-phenyl-amine units giving rise to an intramolecular charge transfer exciton [31, 32]. The emeraldine salt (ES) form of PANi shows three distinct peaks with two new peaks around 430 nm and 800 nm besides the band transition peak around 300 nm, associated with the π -polaron and polaron- π^* band transitions, respectively [30]. The absence of the peak at 430 nm suggests that there is no indication of formation of polaron band deep inside the band gap as reported earlier [30-32] indicating that both the samples are in EB form. The relative intensities of the peaks, however, suggest that the benzenoid units are dominating as compared to the quinoid units more in SF-PNFs.

Both PNFs and SF-PNFs exhibit a distinct photoluminescence peak at 385 nm as shown in Figure 5. However, the intensity of the peak of SF-PNFs is observed to be higher than the PNFs. Leucoemeraldine base (LB) form of PANi exhibits a photoluminescence peak at 400 nm associated with the fully reduced benzenoid unit and the photoluminescence of PANi is quenched if the (fully reduced) benzenoid unit are situated adjacent to a (fully oxidized) quinoid unit [33, 34]. The disappearance of photoluminescence in EB form of PANi is generally attributed to the fact that the benzenoid and quinoid units in emeraldine base were believed to be located adjacent to each other. Here, we have observed photoluminescence in both PNFs and SF-PNFs, though UV-visible absorption spectroscopy suggests that both the samples are in EB form. This contradiction can be resolved on the basis of the explanations proposed by Shimano *et al.* taking into account a dynamic block co-polymeric structure of PANi with two benzenoid units adjacent to a single quinoid unit [33]. It has been reported that in certain specific condition, EB form of PANi exhibits only a single peak around 400 nm, which is attributed to the benzenoid unit, while the emeraldine salt (ES) form of PANi exhibits another peak around 470 nm attributed to the reduced quinoid unit due to higher degree of doping. Furthermore, the photoluminescence of PANi in LB form was reported to be enhanced [33, 34]. We have also found enhancement in photoluminescence intensity after surface functionalization at 385 nm assigned to the π - π^* transition of the benzenoid unit. During the transformation of EB to ES, the peak around 400 nm begins to disappear while the peak around 470 nm begins to appear prominently [33]. But, no such kind of transformation is observed in our case except the photoluminescence enhancement at 385 nm, suggesting that though the PANi nanofibers are initially in EB form, surface functionalization at neutral

p^H value reduce the quinoid units into benzenoid like structures as discussed in following section with detailed functionalization mechanisms in Figure 9, which is consistent with earlier report [22]. The enhancement in the photoluminescence intensity after surface functionalization is ascribed to increased number of benzenoid like units in the polymer chain due to partial reduction at the imine sites as well as incorporation of functional oxygenated species like CHO, OH in the polymer by functionalization of glutaraldehyde through grafting as shown in Figure 9. The partial conversion of quinoid units into benzenoid units indicates the partial transformation of EB form to the LB form of PANi, which has also been revealed by the UV-Visible spectra analysis. This observation reveals that there is no probability of formation of polaron band in SF-PNFs giving only $\pi-\pi^*$ transition. It is well reported that photoluminescence is more probable if the lowest energy transition is for $\pi^*-\pi$ than $n-\pi^*$ as the molar absorptivity of the former is greater than that of the latter [35, 36, 37]. The photoluminescence enhancement/higher quantum yield of functionalized nanofibers is further supported by overlapping of the absorption spectra of PNFs and glutaraldehyde making the energy transfer more probable [38] as shown in Fig.S3 in ESI.

The recorded FT-IR spectrum of PNFs in Figure 6(a) shows characteristics vibrational bands for PANi, whereas the FT-IR spectrum of SF-PNFs in Figure 6(b) contains some new bands in addition to shifting and broadening of some characteristics vibrational bands of PANi. The broad vibrational bands around 3440 cm^{-1} of PNFs and 3433 cm^{-1} of SF-PNFs are assigned to the N-H stretching vibrations of primary and secondary amines attached to benzenoid units of PANi [39, 40, 42]. The enhancement in intensity and shifting of this band to higher wavenumber for SF-PNFs can be ascribed to the overlapping of O-H stretching vibration of cyclic hemiacetal and oligomeric form of glutaraldehyde in SF-PNFs [42]. The lowering of N-H stretching wavenumber in SF-PNFs reveals the intermolecular hydrogen bonding between amine and hydroxyl group [41]. The absorption bands in the $2868\text{-}2935\text{ cm}^{-1}$ region of PANi due to aromatic C-H stretching shifts to $2861\text{-}2927\text{ cm}^{-1}$ in SF-PNFs with increase in intensity [39, 40, 42]. It indicates the overlapping O-H bending vibration of cyclic hemiacetal or/and oligomeric form of glutaraldehyde [42]. A sharp peak with medium intensity, unlike the pristine PNFs, at 1720 cm^{-1} for SF-PNFs attributed to C=O stretching vibration of non conjugated aldehyde confirms the presence of monomeric glutaraldehyde [42]. The weak absorption band at 1636 cm^{-1} of PNFs is attributed to C=N aromatic stretching vibrations in quinoid units, which converts into a strong and broad one at 1639 cm^{-1} in SF-PNFs. This can be simultaneously attributed to C=O stretching vibrations in amide

bond and C=N stretching vibrations in Schiff base formed between aldehyde group of monomeric glutaraldehyde and primary amine of PNFs [41, 42]. The strong absorption bands, appearing at 1582 cm^{-1} in the vibration spectra of PNFs and SF-PNFs are assigned to C=C stretching vibration of quinoid units of PAni [39, 40, 42]. The appearance of vibrational bands in the region $1442\text{--}1502\text{ cm}^{-1}$ PNFs is due to characteristics C=C stretching vibrations of benzenoid units in PAni, however, it shifts to 1504 cm^{-1} for SF-PNFs with relatively higher intensity. The weak band at 1234 cm^{-1} in PNFs corresponding to various stretching and bending vibrations of C-C bond, has been observed to be upshifted to 1240 cm^{-1} in SF-PNFs. The strong peak at 1306 cm^{-1} along with a small shoulder peak at 1370 cm^{-1} in the FTIR spectrum of PNFs belongs to the characteristic of C-N stretching vibrations, related to aromatic amine [40, 41]. The sharp splitting and shifting of these two peaks in SF-PNFs to lower wavenumber region $1304\text{--}1354\text{ cm}^{-1}$ with increase in intensity indicates possible interaction of cyclic hemiacetal forms of glutaraldehyde with amine and imine sites of PNFs through covalent bonding. The intense bands at $1054\text{--}1114\text{ cm}^{-1}$ in PNFs, associated with C-H in plane bending vibrations, shift to $1048\text{--}1145\text{ cm}^{-1}$ region [39, 40, 42]. This change can be attributed due to overlapping of O-H bending vibrations. The weak absorption band seen at 818 cm^{-1} of PNFs shifts to lower frequency region for SF-PNFs into 812 cm^{-1} indicating an increase of degree of oxidation of para-disubstituted benzene after functionalization [39, 40].

In ^1H NMR spectrum of PNFs in deuterated dimethyl sulfoxide (DMSO) as shown in Figure 7, a strongest peak broad is observed centred at 6.9 ppm is due to the protons in the benzenoid units [43-47]. A doublet of unequal strength observed at 7.6-7.8 ppm is associated with disubstituted phenylene i.e., quinoid units [43-45]. The relatively higher peak area corresponding to the protons of benzenoid units than the protons in quinoid units indicates higher no. of benzenoid units than the quinoid units in the polymer chain which is also suggested by UV-visible and photoluminescence results as discussed above. A sharp peak of medium strength appeared at 6.2 ppm corresponds to end primary amine group attached with benzene ring adjacent to a secondary amine which is also attached with another benzene unit [43-47]. The characteristic peak of unprotonated secondary amine (-NH) within the polymer chain appears at 4.6 ppm [43-47]. Generally, ES form of PAni shows three equally spaced peaks of equal strength in the region 6.9-7.3 ppm in ^1H NMR spectrum as a result of protonated -NH resonance due to the ^{14}N with unit spin which makes the proton attached to it split into three lines as reported earlier [43, 44]. It is possible only if proton exchange process is much slower. It has been also reported that proton exchange process becomes

slower in ammonium ion [41]. Moreover, another weak peak is observed for ES form of PANi due to hydrogen bonding between water and H-N^+ [43, 44]. Ultimately, the absence of the sharp and equidistant triplet of equal strength in the range 6.9-7.3 ppm and the single small peak in the region 8 ppm reveals that the PNFs are in EB form, which supports our earlier reported result.

It has been observed that the ^1H NMR signals due to the aromatic protons of PANi chain after surface functionalization shift towards upfield as compared to pristine suggesting deprotonation of PANi chain after functionalization as shown in Figure 8 [44]. Interestingly, the intensity of the signal at 4.6 ppm associated with unprotonated secondary amine ($-\text{NH}$) is found to be decreased in SF-PNFs as compared to pristine PNFs, which indirectly indicates the oxidation (loss of hydrogen as shown in Figure 9) of the secondary amine within the polymer chain during the conjugation with hydroxyl (in case of cyclic hemiacetal) or aldehyde (in case of monomeric form) group of glutaraldehyde. Conjugation of cyclic hemiacetal or/and oligomeric form of glutaraldehyde is also supported by the appearance of two prominent NMR signals in the range 4.7-4.9 ppm in the ^1H NMR spectrum of SF-PNFs. These new peaks are attributed to the protons in cyclic hemiacetal or/and oligomeric form of glutaraldehyde which is in close environment to oxygen as shown in predicted chemical structure of SF-PNFs in Figure 8. More interestingly, the signals assigned to end primary amine group attached to benzenoid unit at 6.2 ppm in PNFs are found to be completely disappeared after surface functionalization. It is due to the fact that glutaraldehyde has significantly higher reactivity towards primary amine [48]. This confirms that primary amine groups present at the end terminals of polyaniline have been utilized in Schiff base formation during the conjugation with monomeric glutaraldehyde, which is shown with detailed reaction mechanisms in Figure 9. The appearance of another new peak at 9.7 ppm in SF-PNFs attributed to aldehyde ($-\text{CHO}$) group, further confirms the presence of monomeric glutaraldehyde.

The effect of functionalization on PNFs on optical properties in acidic condition has been reported in our earlier report [22]. However, the effect is slightly different in neutral condition as we have studied so far. It is in the sense that surface functionalization in acidic condition revealed a transition of EB towards ES form of polyaniline as reported earlier, while in the present work it is observed that surface functionalization causes a partial transition of EB form of PANi into LB form. Considering the results obtained so far by UV-visible, photoluminescence, FT-IR and ^1H NMR spectroscopy, we have proposed a detailed

functionalization mechanism of PNFs by glutaraldehyde. The possible functionalization mechanism is shown in Figure 9 and tries to cover all the outcomes obtained till now.

3.5. Enhancement in surface free energy and surface polarity after surface functionalization

Table I: Average contact angle values of water, ethylene glycol and diiodomethane on pristine and surface functionalized PANi films.

Material	Water Contact angle (°)	Ethylene Glycol Contact angle (°)	Diiodomethane Contact angle (°)
PNFs	76.2 ± 0.8	60.2 ± 0.2	34.6 ± 1.3
SF-PNFs	52.1 ± 0.3	40.7 ± 0.8	37.2 ± 1.8

Table II: Surface energy and its components calculated by the OWRK method taking water and diiodomethane as probe liquids.

Material	OWRK method			
	γ_s^d mNm ⁻¹	γ_s^p mNm ⁻¹	γ_s mNm ⁻¹	% Polarity
PNFs	42.19	4.29	46.48	9.30
SF-PNFs	40.96	12.19	53.15	22.93

Table III: Surface energy and its components calculated by AB method taking water, ethylene glycol and diiodomethane probe liquids.

Material	AB method					
	γ_s^{LW} mNm ⁻¹	γ_s^- mNm ⁻¹	γ_s^+ mNm ⁻¹	γ_s^{AB} mNm ⁻¹	γ_s mNm ⁻¹	% Polarity
PNFs	42.19	13.50	0.73	6.27	48.46	12.93
SF-PNFs	40.96	32.87	0.64	9.17	50.13	18.30

It was reported earlier that surface properties of a material like wettability which is an important phenomenon for binding or adherence between two materials, can be evaluated by calculating surface energy of that material using contact angle values of different polar and apolar test liquids on it [23, 24]. Usually, the high energy surfaces due to nature of the chemical bonds (viz. covalent, ionic) hold them together, possess higher wettability. Thus, the presence of chemical groups present on the surface of a material defines the wettability, which is one of the most prerequisite parameters correlated with cell-biomaterial interfacial interactions. So far as, we have demonstrated directly the incorporation polar functional groups onto the surface of PNFs with the help of FT-IR and NMR spectroscopy, there are no such direct method to calculate the total surface energy or surface tension except some indirect or semi-empirical methods.

Contact angle values of PNFs before and after surface functionalization with glutaraldehyde with three different test liquids are shown in Table I. Decrease in water contact angle value upto 52.1° after functionalization reveals the improved wettability of the material surface.

Total Surface energy (γ_s) along with its dispersive (γ_s^d) and polar (γ_s^p) components using two test liquids water/ethylene glycol and diiodomethane by OWRK method have been presented in Table II. It was established earlier that increase in the value of polar component of surface energy indicates the increase in the concentration of polar groups on the polymer surface [49]. It has been found that the total surface energy value after functionalization is increased significantly from 46.48 mNm⁻¹ to 53.15 mNm⁻¹. This reveals enhancement in

wettability of the functionalized surface. Also, the increase in polar component (12.19 mNm^{-1}) after surface functionalization has proved indirectly the incorporation of polar functional groups like hydroxyl and aldehyde groups through glutaraldehyde onto the surface of PNFs. It is also to be noted that the presence of a small value of polar component of surface energy but not readily negligible, in case of pristine PNFs can be assigned to the available polar groups like primary and secondary amines in the polymer chains and thereby hydrophilicity of the surface is enhanced.

Furthermore, surface energy calculations of PNFs before and after surface functionalization are also performed by AB method using three test liquids: water, ethylene glycol and diiodomethane and presented in Table III. One of the major advantages of this method over the earlier one is that it can provide a complete scenario along with acidic and basic character of the surface beyond the total surface energy and dispersive-polar components. In fact, the “polar” term designate three classes of compound viz. hydrogen bonding compounds, dipolar compounds and the compounds that interact with Lewis acid and base [49, 50]. This AB method reported by Van oss et al., distinguishes this acid base interactions as a component of surface energy denoted by γ^{AB} . The results obtained from this method differ slightly from OWRK method though the results of both the methods can be correlated as the enhancement in total surface energy and its polar component can be observed in both cases. As seen from Table III, the Lifshitz-Van der Waals components of PNFs after surface functionalization significantly decreased to 40.96 mNm^{-1} from 42.19 mNm^{-1} , which is also evident from OWRK method. But, the most important observation is the increase in acid-base components of surface energy after surface functionalization which ultimately points to the improved hydrophilicity of the surface. To speak more specifically, the Lewis base component (γ_s^-) of SF-PNFs is enhanced by a large difference than the PNFs as observed in Table III, which indicates the improved basic character of functionalized surface. This can be attributed due to the hydroxyl and aldehyde functional groups introduced onto the surface through covalent bonding between glutaraldehyde and PANi. The concept of possible covalent bonding between glutaraldehyde and amine groups of PANi is more evident from the enhancement in acid-base component of surface energy, which signifies proton and electron donating character of surface as discussed in section 3.4.

The enhancement in total surface energy value along with polar components specifically Lewis base component value after surface functionalization is correlated to the biocompatibility assessment of surface functionalized samples in the following sections.

3.6. Membrane stability test

It has been observed that SF-PNFs show significantly very less haemolysis as compared to the pristine samples as shown in Figure 10. The surface functionalized samples are found to exhibit haemolysis activity less than one percentage and hence, they are non-haemolytic. The percentage of haemolysis of all the samples is compared with the haemolysis activity of ascorbic acid, also known as Vitamin C. Ascorbic acid is an organic compound having tremendous antioxidant properties. More interestingly, SF-PNFs are also found to exhibit haemolysis activity very similar to the ascorbic acid in presence of Triton X-100, which is generally used to lyse cells to extract protein or organelles, or to permeabilize the membranes of living cells. Therefore, this observation reveals that surface functionalization of PNFs renders stability towards cell membrane. Not only this, it also indirectly indicated to the improved antioxidant property of SF-PNFs. However, antioxidant property of PANi is quite expected as several researchers have already reported this property of PANi [51-54]. But, it is important to note in this work that enhancement of membrane stability property as well as antioxidant property of SF-PNFs is caused only by surface functionalization by glutaraldehyde and it is clearly seen from Fig.11, when compared with the haemolysis activity of pristine PNFs.

3.7. MTT assay

The results as shown in Figure 11 indicate that surface functionalization increases the cell viability more than two times than the control and pristine samples. It is also observed quite noticeably that cell viability increases with increase in the concentration of the samples. This improved cell viability can be strongly correlated with the results obtained by FT-IR, NMR techniques as well as surface energy calculations.

In normal cell mechanisms, protein adsorption is the determining step in the first phase during cell biomaterial interaction for controlling cell viability. Moreover, the type of adsorbed protein layer and their orientations are related to the surface properties especially to surface energy [55]. It has been also proved that the polar component of surface energy and Lewis basicity play a key role in interfacial interactions between cell and biomaterials leading

to surface biocompatibility [56]. Although, the very low and very high values of these components are not suitable for cellular activities, the values reported in this work are found to be quite utile for improved cell viability. Therefore, SF-PNFs are expected to act as an artificial ECM for PBMC cell line, which can possibly provide cell mediator growth factors through interaction with integrin proteins like collagen, fibronectin, laminin etc due to improved hydrophilicity and wettability achieved by functionalization by glutaraldehyde. Similar kind of correlation between the surface properties of a material and its cell behavior has been reported already by other researchers.

4. Experimental

4.1. Materials

Aniline (p.a. Merck) was distilled under reduced pressure before use. Ammonium peroxydisulfate (p.a. Merck) and Hydrochloric acid (Rankem) were used without further purification. Deionised water (12 MΩ cm) used for the synthesis was obtained from a Milli-Q system. 25% solution of Glutaraldehyde (p.a. Merck) was diluted to 1% using Milli-Q water. All other chemicals and reagents were of analytical grade and used as received.

4.2. Synthesis of polyaniline nanofibers

Polyaniline nanofibers (PNFs) were synthesized using dilute polymerization method described by N. R. Chiou [26, 27], where polymerization of aniline has been carried out at a substantially lower concentration in presence of protonic acid as described below as compared to the conventional polymerization methods:

A solution of 1M HCl (dopant acid) was prepared and the monomer aniline was dissolved in a small portion of that solution. Ammonium peroxydisulfate (oxidizing agent) was dissolved in the remaining portion of the dopant acid solution. The initial concentration of aniline in the reaction mixture was kept at 8 mM and the molar ratio of the monomer to the oxidant was maintained at 2:1. The monomer solution was then carefully transferred to the solution of APS. The reaction was allowed to take place in a magnetic stirrer at a very slow stirring rate at room temperature for about 24 h till the whole mixture became dark green. The whole mixture was then filtered and washed with deionised water and methanol for several times. For the purpose of film preparation, emeraldine base (EB) form of PANi has been obtained by further washing the mixture by 15% ammonia solution followed by several times with deionised water until the filtrate became colourless. PANi films were prepared as

reported earlier [57]. Typically, 500 mg of finely ground PNFs has been magnetically stirred in 30 ml of NMP solution for 8 h after which the intense blue solution was again sonicated so that the PNFs become completely dissolved. A pasteur pipette was used to cast the films on clean glass slides from this solution. The casted glass then dried in an oven at 60°-70°C for 4 h and after drying, films can be removed by immersing the glass slides in water for 5-10 min.

4.3. Surface functionalization of polyaniline nanofibers

Surface Functionalization was accomplished by treating the purified PNFs with 1% glutaraldehyde solution for a period of 24 h. Subsequently, the surface functionalized polyaniline nanofibers (SF-PNFs) were washed with deionised water to remove the excess glutaraldehyde. The reason for choosing glutaraldehyde as a surface functionalization agent was its high reactivity towards the amine group [48] and as such it has been often used as a cross-linking agent. The different molecular forms of glutaraldehyde in aqueous solution enable it to cross-link two materials having active amine groups [48].

4.5. Analytical techniques

The structural, morphological and conformational characterizations of PNFs and SF-PNFs were accomplished using different characterization techniques as described below. Transmission electron microscopy was accomplished using a JEOL JEM 200 CX transmission electron microscope (TEM) installed at SAIF, NEHU, Shillong. Morphological characterizations were carried out using Field emission scanning electron microscopy (FESEM) at IASST, Guwahati, India. The thermal stability study was performed by a Perkin Elmer model STA 6000 thermal analyzer with a dynamic nitrogen flow of 20 ml min⁻¹ to avoid mass increase due to oxidation. FTIR spectra were recorded using a Perkin Elmer spectrum 100 FTIR spectrometer. ¹H NMR spectra of samples have been recorded using 400 MHz NMR spectrophotometer from Jeol to obtain detailed structural informations about the polymer before and after functionalization. The optical properties were investigated employing UV-Vis absorption and Photoluminescence spectroscopy. Contact angle measurement of PANi films before and after surface functionalization were carried out using contact angle measurement system from Data physics instrument GmbH, Germany, model OCA 15 EC. Contact angles of two polar liquids: water and ethylene glycol and a non polar liquid: diiodomethane, were measured using sessile drop method on PANi films before and after modification at room temperature. Contact angle data has been recorded three times for each liquid and here, the averages of those have been presented with S.D.

5. Conclusions

The surface of PNFs has been successfully functionalized with glutaraldehyde with a view to enhance its surface properties by introducing bioactive species that can promote membrane stability property and viability for PBMC cell line or lymphocytes. TEM and FESEM images confirm the formation of nanofibers of polyaniline, whereas spectroscopic techniques like UV-visible and photoluminescence spectroscopy reveal that both pristine and functionalized samples are in EB form. Thermogravimetric analysis indicates actual glutaraldehyde mass fraction introduced on the surface of PNFs is about 1% of total weight of the polymer. It further revealed improved thermal stability of PNFs after functionalization. FT-IR and ¹H NMR spectroscopic analysis confirm the incorporation of polar hydroxyl (-OH) and aldehyde (-CHO) functional groups onto to the surface of PNFs leading to the improved hydrophilicity after functionalization. Surface energy calculations with the help of contact angle data by both OWRK and AB method proved the enhancement in total surface energy along with its polar components after surface functionalization. Increase in Lewis basicity component of SF-PNFs achieved by AB method ultimately leads to surface biocompatibility of the material, which has been confirmed by the biocompatibility assessments with the help of membrane stability test and MTT assay. Membrane stability test shows negligible haemolysis activity of SF-PNFs similar to Vitamin C (Ascorbic acid). It also indirectly indicates to the improved antioxidant property of PNFs after surface functionalization. The other important observation is the improved viability of PBMC cell line towards SF-PNFs more than twice than that of the control without any immune response from the cells. Polyaniline nanofibers functionalized with glutaraldehyde can be a suitable biomaterial for various biomedical applications like tissue engineering, drug delivery and enzyme immobilization for biosensing applications.

6. Acknowledgement

The authors gratefully acknowledge the financial assistance provided by DST through Inspire fellowship scheme. Help extended by the staff of the Electron Microscopy Division, SAIF, Shillong for TEM and Scanning Electron Microscopy Division, CIF, IASST SEM measurement has been cordially acknowledged.

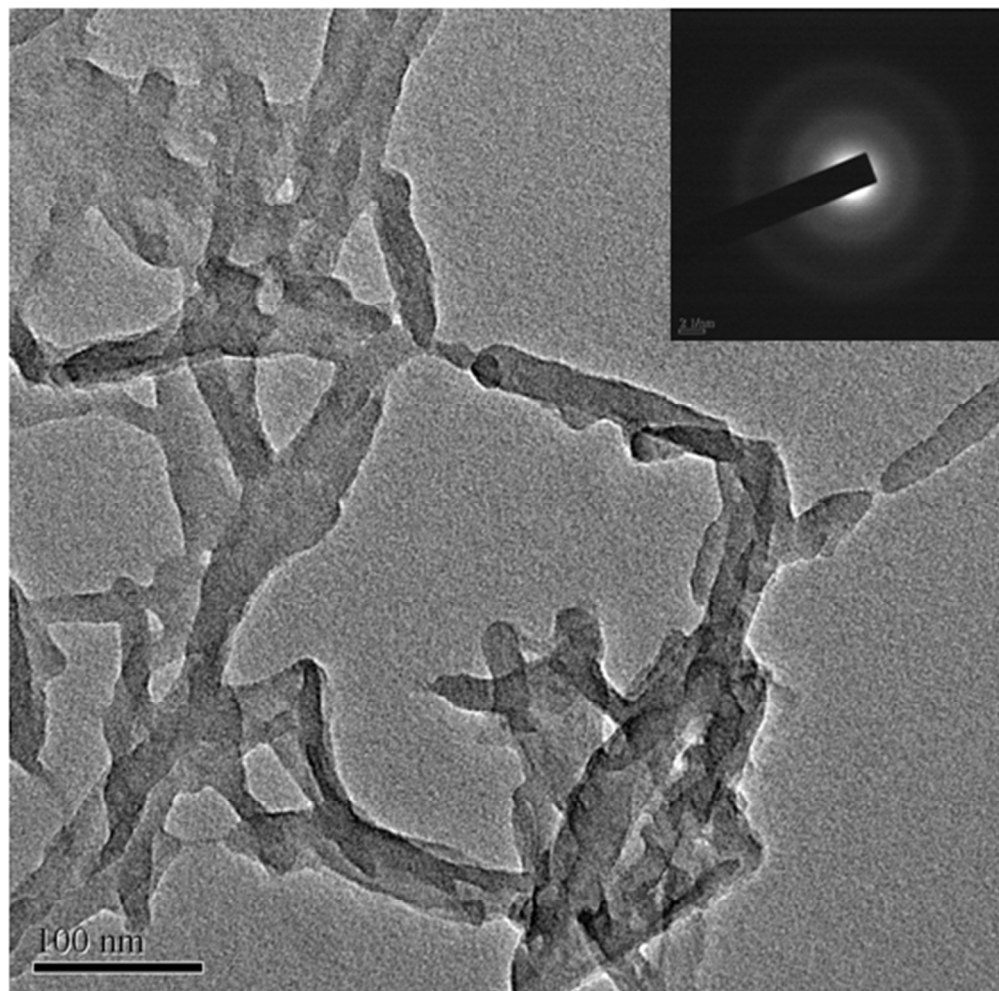
7. References

1. Y. Sharma, A. Tiwari, S. Hattori, D. Terada, A. K. Sharma, M. Ramalingam and H. Kobayashi, *Int. J. Biol. Macromol.*, 2012, 51, 627– 631.

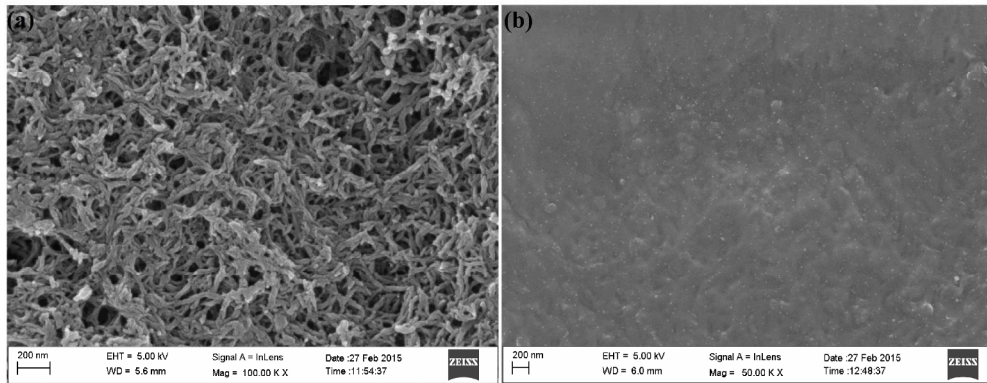
2. I. S. Chronakis, S. Grapenson and A. Jakob, *Polymer*, 2006, 47, 1597–1603.
3. L. G. Mobarakeh, M. P. Prabhakaran, M. Morshed, M. Nasr-Esfahani, H. Baharvand, S. Kiani, S. S Al-Deyab and S. Ramakrishna, *J. Tissue Eng Regen Med*, 2011, 5, e17–e35.
4. R. Ravichandran, S. Sundarrajan, J. R. Venugopal, S. Mukherjee and S. Ramakrishna, *J. R. Soc. Interface*, 2010, DOI:10.1098/rsif.2010.0120.
5. R.H. Baughman, *Synth. Met.*, 1996, 78 (3), 339–353.
6. N. K. Guimard, N. Gomez and C. E. Schmidt, *Prog. Polym. Sci.*, 2007, 32, 876–921.
7. A. D. Bendrea, L. Cianga and I. C. Dya, *J. Biomater. App.*, 2011, 26.
8. T. H. Qazi, R. Rai and A. R. Boccaccini, *Biomaterials*, 2014, 35, 9068–9086.
9. Mattioli-Belmonte, M., Giavaresi, G., Biagini, G., Virgili, L., Giacomini, M., Fini, M., et al. *Int. J. Artif. Organs.*, 2003, 26, 1077–1085.
10. James M Anderson, *Annu. Rev. Mater. Res.*, 2001, 31, 81–110
11. Z. Ma, Z. Mao and C. Gao, *Colloids and Surfaces B: Biointerfaces*, 2007, 60, 137–157.
12. L. Dai and A. W. H. Mau, *J. Phys. Chem. B*, 2000, 104, 1891–1915.
13. J.M. Goddard and J.H. Hotchkiss, *Prog. Polym. Sci.*, 2007, 32, 698–725.
14. T. Kobayashi, H. Yoneyama and H. Tamura, *J. Electroanal. Chem.*, 1984, 161, 419–423.
15. K.S. Ryu, K. M. Kim, Y. J. Park, N. G. Park, M. G. Kang and S. H. Chang, *Solid State Ionics*, 2002, 152–153, 861–866.
16. E. W. Paul, A. J. Ricco and M. S. Wrighton, *J. Phys. Chem.*, 1985, 89 (8), 1441–1447.
17. S. Ameen, M. S. Akhtar, Y. S. Kim, O. Yang and H. S. Shin, *J. Phys. Chem. C*, 2010, 114, 4760–4764.
18. R. Garjonyte and A. Malinauskas, *Biosensors and Bioelectronics*, 2000, 15, 445–451.
19. E. Smela, *Adv. Mater.*, 2003, 15 (6), 481–494.
20. H. J. Choi and M. S. Jhon, *Soft Matter*, 2009, 5, 1562–1567.
21. Y. D. Liu, H. Y. Kim, J. E. Kim, I. G. Kim, H. J. Choi and S. J. Park, *Mater. Chem. Phys.*, 2014, 147, 843–849.
22. R. Borah, S. Banerjee and A. Kumar, *Synth. Met.*, 2014, 197, 225–232.
23. D. K. Owens and R. C. Wendt, *J. App. Polym. Sci.*, 1969, 13, 1741–1747.
24. C. J. Van Oss, D. R. Absolom and A.W. Neumann, *Colloids and Surfaces*, 1980, 1, 45–56.
25. C. J. Van Oss, M. J. Roberts, R. J. Good and M. K. Chaudhury, *Colloids and Surfaces*, 1987, 23, 369–373.
26. N. R. Chiou, Ph. D. Thesis, The Ohio State University, 2006.
27. N. R. Chiou, A. J. Epstein, *Adv. Mater.*, 2005, 17, 1679–1683.
28. Y. Wei and K. F. Hsueh, *J. Polym. Sci. Part A: Polym. Chem.*, 1989, 27, 13, 4351–4363.
29. Y. Wei, G. W. Jang, K. F. Hsueh, E. M. Scherr, A. G. MacDiarmid and A. J. Epstein, *Polymer*, 1992, 33, 2, 314–322.
30. S. Stafstrom, J. L. Brédas, A. J. Epstein, H. S. Woo, D. B. Tanner, W. S. Huang and A. G. MacDiarmid, *Phys. Rev. Lett.*, 1987, 59 (13), 1464–1467.
31. J. Wu, Ph. D. Thesis, Characterisation and applications of conducting polymer coated textiles, University of Wollongong, 2004.
32. M. Amrithesh, Ph. D. Thesis, Investigations on some selected conducting polymers and polymer composites for possible optoelectronic applications; Cochin University of Science and Technology, 2009.

33. J. Y. Shimano and A. G. MacDiarmid, *Synth. Met.*, 2001, 123, 251-262.
34. J. R. G. Thorne, J. G. Masters, S. A. Williams, A. G. MacDiarmid and R. M. Hochstrasser, *Synth. Met.*, 1992, 49, 159.
35. D. A. Skoog, S. R. Crouch and F. J. Holler, *Principles of Instrumental Analysis*, 6th edn., Thomson Brooks/Cole., 2007.
36. D. C. Harris and M. D. Bertolucci, *Symmetry and Spectroscopy: An introduction to Vibrational and Electronic Spectroscopy*, 1st edn, Dover Publications, New York, 1989.
37. F. Liu, T. Wu, J. Cao, H. Zhang, M. Hu, S. Sun, F. Song, J. Fan, J. Wang and X. Peng, *Analyst*, 2013, 138, 775.
38. P. Yang, M. M. Yang and B. S. Yang, *Chinese Journal of Chemistry*, 1996, 14, 2, 109-113.
39. N. S. Sariciftci, H. Kuzmany, H. Neugebauer and A. Neckel, *The Journal of Chemical Physics*, 1990, 92, 4530.
40. Y. Furukawa, F. Ueda, Y. Hyodo, I. Harada, T. Nakajima and T. Kawagoe, *Macromolecules* 1988, 21, 1297-1305.
41. D. L. Pavia, G. M. Lampman and G. E. Kriz, *Introduction to spectroscopy*, 4th edition, 2008.
42. S. Quillard, G. Louarn, S. Lefrant, and A. G. MacDiarmid, *Phys. Rev. B*, 1994, 50, 12496.
43. R. Abdelkader, H. Amine and B. Mohammed, *World Journal of Chemistry*, 2013, 8 (1), 20-26.
44. X. Wang, T. Sun, C. Wang, C. Wang, W. Zhang and Y. Wei, *Macromol. Chem. Phys.*, 2010, 211, 1814-1819.
45. I. Mav and M. Zigon, *Polymer Bulletin*, 2000, 45, 61-68.
46. R. Mathew, B. R. Mattes and M. P. Espe, *Synth. Met.*, 2002, 131, 141-147.
47. Y. Cao, S. Li and Z. D. Guo, *Synth. Met.*, 1986, 16, 305-315.
48. I. Migneault, C. Dartiguenave, M. J. Bertrand and K. C. Waldron, *Bio Techniques*, 2004, 37, 790-802.
49. P. M. Lopez-Perez, A. P. Marques, R. M. P. da Silva and I. P. R. L. Reis, *J. Mater. Chem.*, 2007, 17, 4064-4071.
50. G. Bayramoğlu, A. U. Metin and M. Y. Arica, *Applied Surface Science*, 2010, 256, 6710-6716.
51. J. Wang, L. H. Zhu, J. Li and H. Q. Tang, *Chinese Chemical Letters*, 2007, 18, 1005-1008.
52. M. G. Nikolaidis, J. T. Sejdic, P.A. Kilmartin, G.A. Bowmaker and R.P. Cooney, *Current Applied Physics*, 2004, 4, 343-346.
53. J. P. Saikia, S. Banerjee, B. K. Konwar and A. Kumar, *Colloids and Surfaces B: Biointerfaces*, 2010, 81, 158-164.
54. S. Banerjee, J. P. Saikia, A. Kumar and B. K. Konwar, *Nanotechnology*, 2010, 21, 045101.
55. E. Ostuni, R. G. Chapman, R. E. Holmlin, S. Takayama and G. M. Whitesides, *Langmuir*, 2001, 17, 5605-5620.
56. D. H. Kaelble and J. Moacanin, *Polymer*, 1977, 18, 475-482.

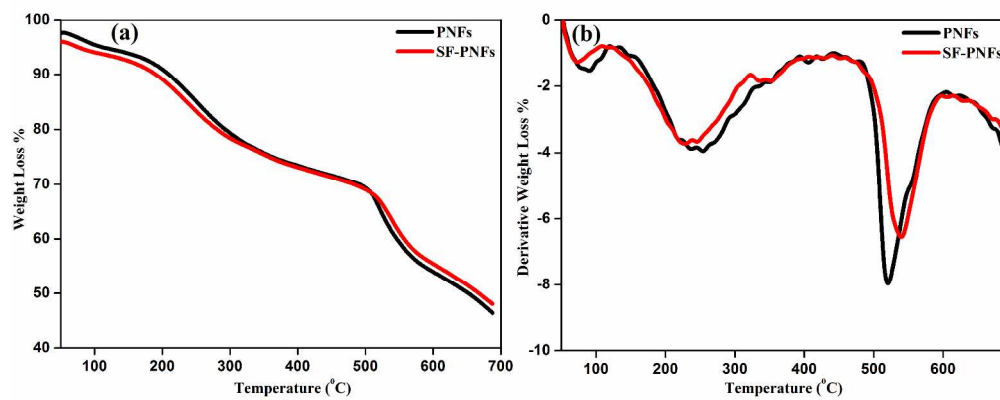
57. M. Angelopoulos, G. E. Asturias, S. P. Ermer, A. Ray, E. M. Scherr, A. G. MacDiarmid, M. Akhtar, Z. Kiss and A. J. Epstein, *Molecular Crystals and Liquid Crystals Incorporating Nonlinear Optics*, 1988, 160, 1, 151-163.



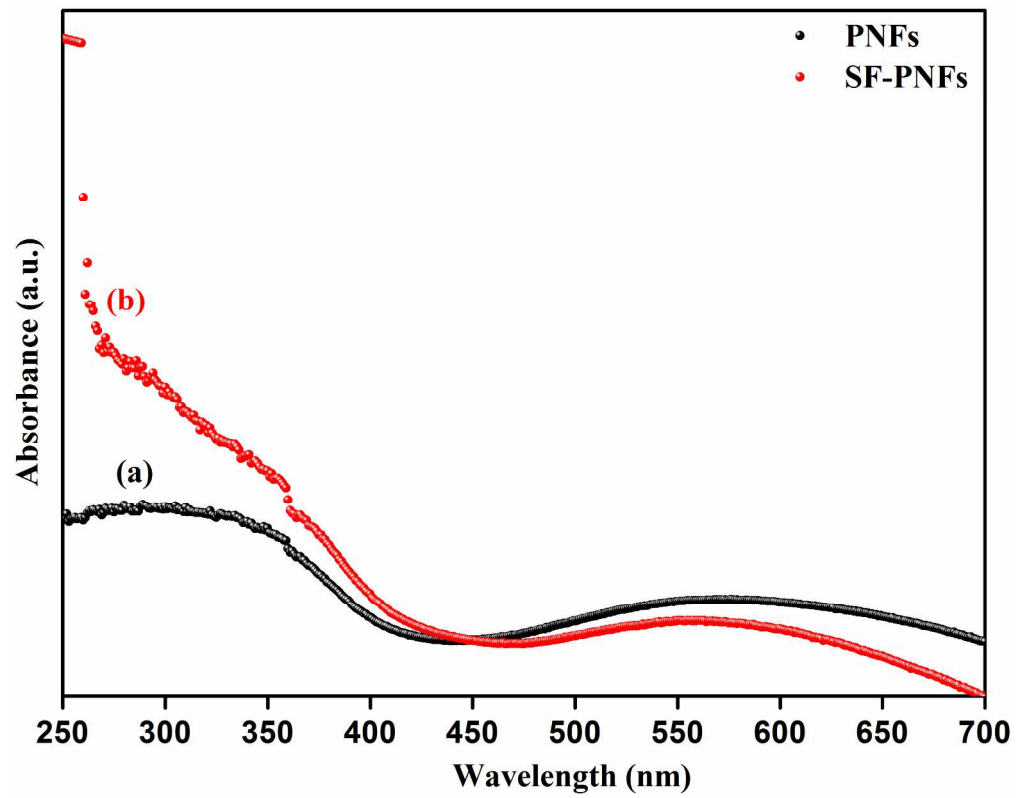
Transmission electron micrograph of PNFs with SAED pattern (inset)
138x137mm (96 x 96 DPI)



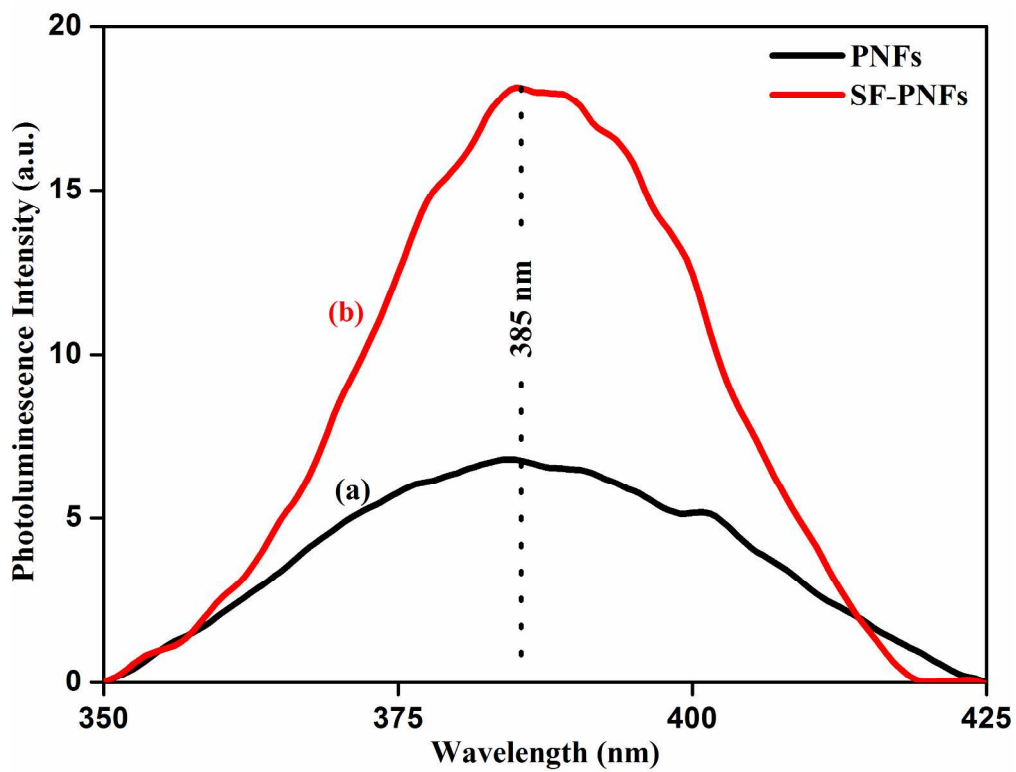
FESEM image of PNFs in (a) powder form and (b) film form
296x209mm (300 x 300 DPI)



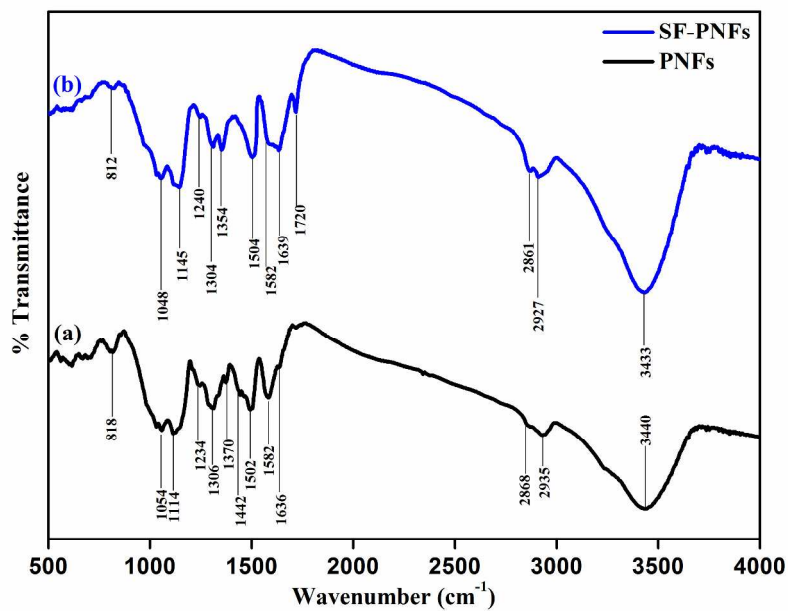
(a) TGA thermograms and (b) DTG plots of PNFs and SF-PNFs
296x209mm (300 x 300 DPI)



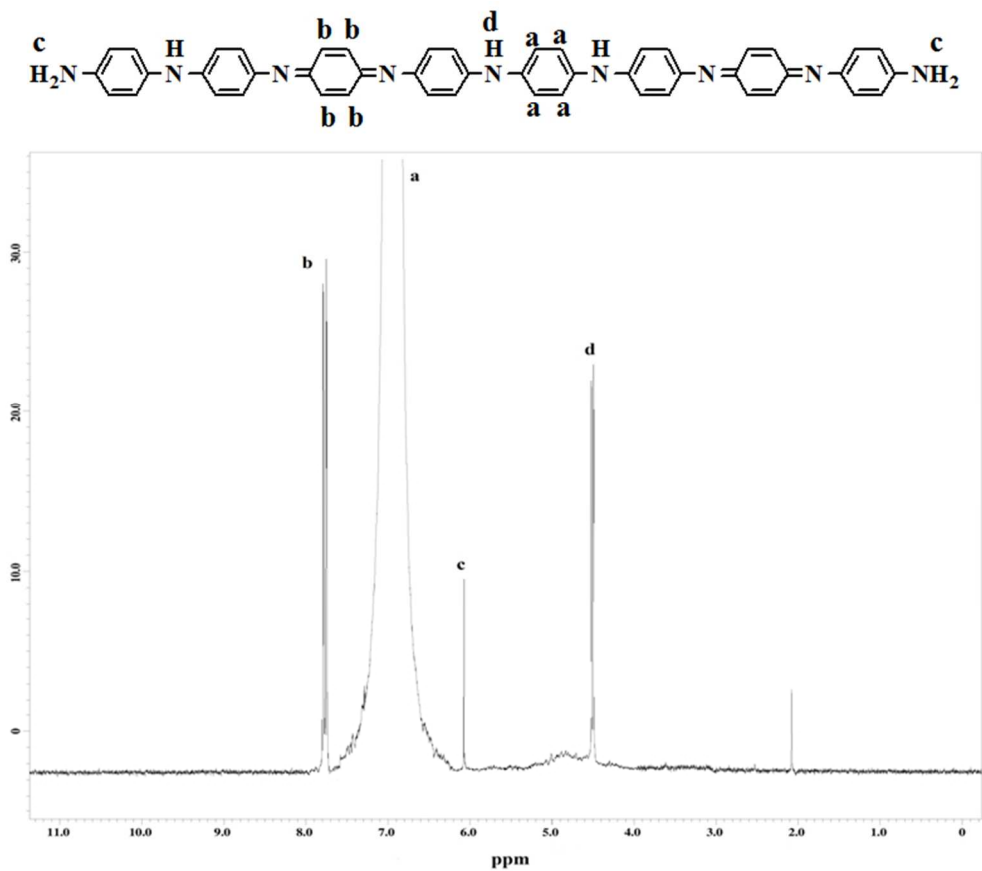
UV-visible absorption spectra of (a) PNFs and (b) SF-PNFs in 0.1M PBS at pH =7.4
219x177mm (300 x 300 DPI)



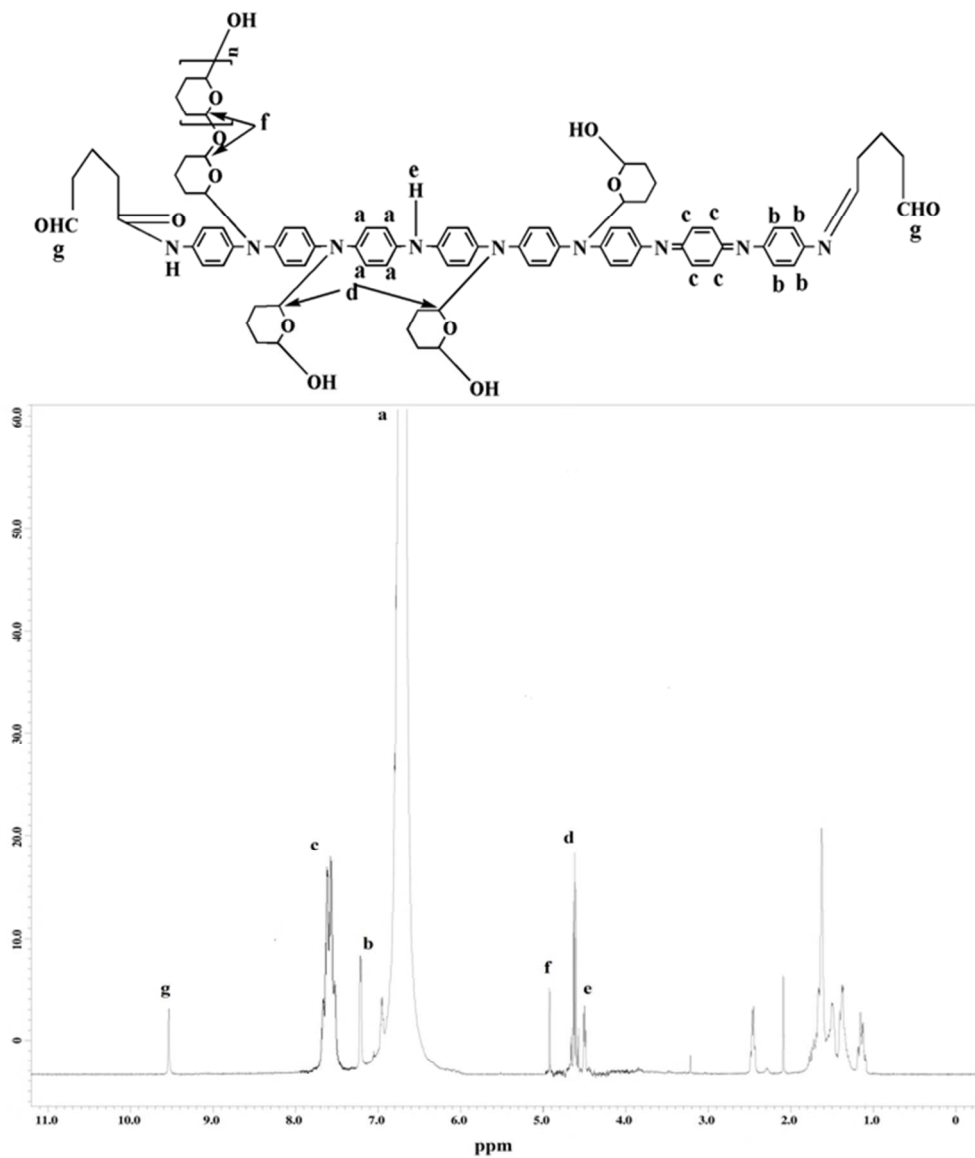
Emission spectra of (a) PNFs and (b) SF-PNFs in 0.1M PBS at pH =7.4 (λ_{exc} =280 nm)
229x177mm (300 x 300 DPI)



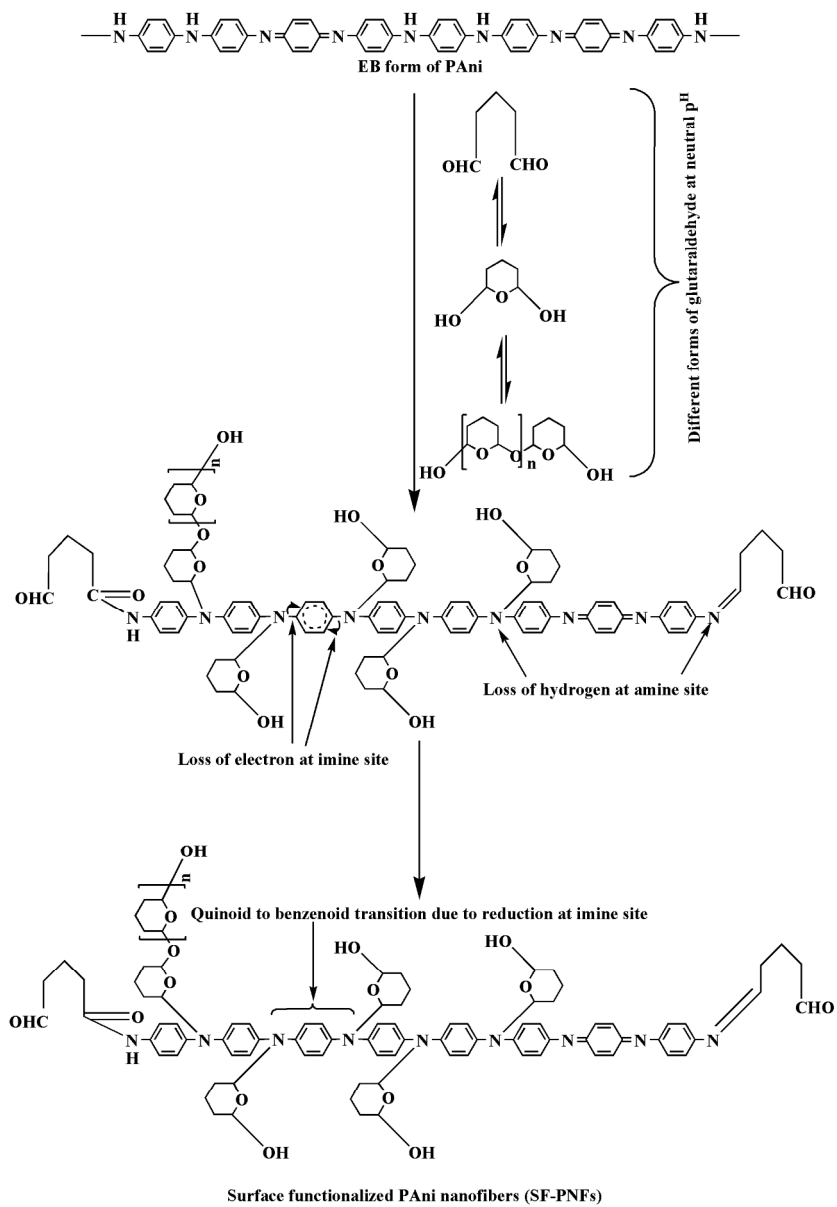
Vibrational spectra of polyaniline nanofibers (PNFs) (a) before and (b) after surface functionalization showing incorporation of polar functional hydroxyl (-OH) and aldehyde (-CHO) groups
296x209mm (300 x 300 DPI)



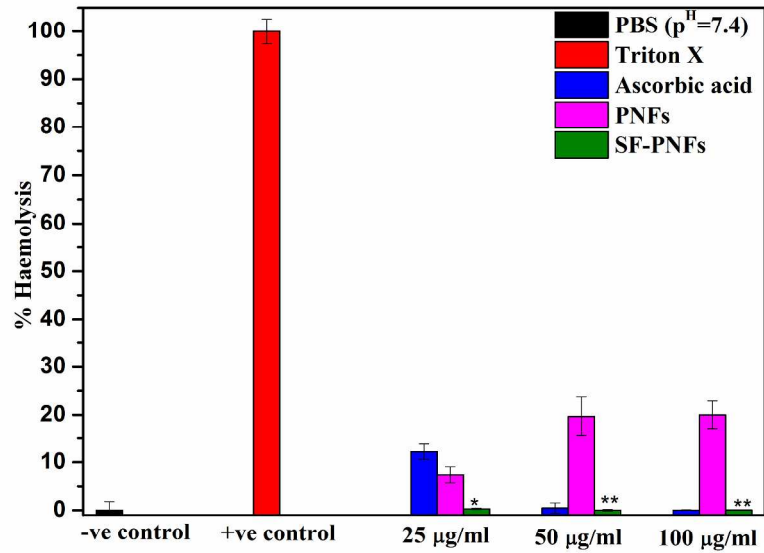
¹H NMR spectrum showing the characteristics peaks of EB form of PNFs. Observed peaks are assigned by labelling the various protons in different chemical environment in predicted chemical structure of the polymer
210x191mm (96 x 96 DPI)



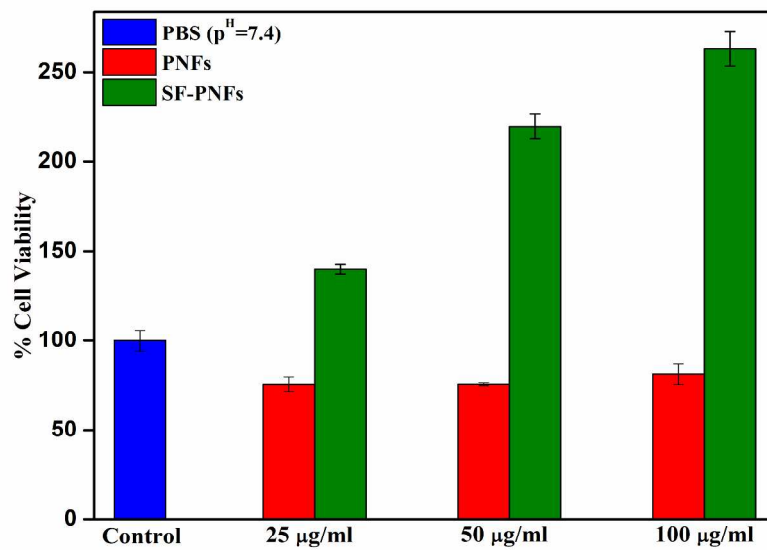
¹H NMR spectrum of SF-PNFs showing the chemical shift value after incorporation of hydroxyl (-OH) and aldehyde (-CHO) functional groups. Observed peaks are assigned by labelling with the help of predicted chemical structure of the polymer
192x222mm (96 x 96 DPI)



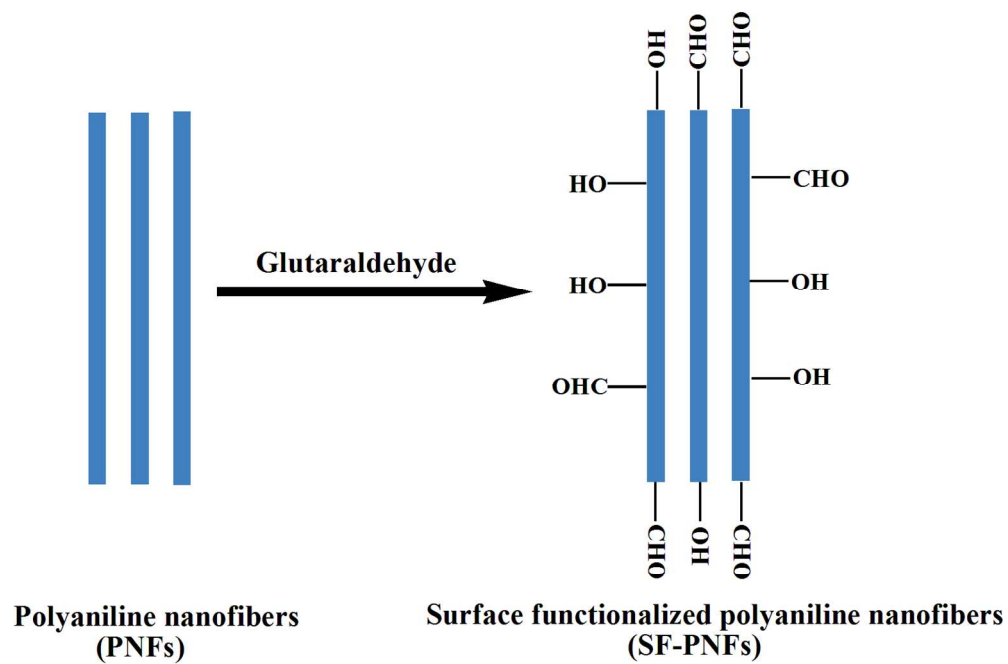
Scheme of possible functionalization mechanisms of PNFs by three different forms of glutaraldehyde showing quinoid to benzenoid transformation in the polymer chain
168x243mm (300 x 300 DPI)



Haemolysis activity of PNFs and SF-PNFs in terms of percentage of haemolysis in PBS at pH =7.4 showing a comparison of haemolysis activity of drug ascorbic acid. Data are expressed as means \pm SD, n=3; **: $P \geq 0.001$, values are significantly different from those obtained with +ve control
296x209mm (300 x 300 DPI)



Percentage of cell viability of PBMC cell line on PNFs and SF-PNFs. Absorbance data were recorded at 570 nm after 24 h and expressed as means of % cell viability \pm SD for n = 4.
296x209mm (300 x 300 DPI)



Schematic representation of surface functionalization of PNFs by glutaraldehyde
141x94mm (300 x 300 DPI)